Proceedings of the XVII ECSMGE-2019
Geotechnical Engineering foundation of the future
ISBN 978-9935-9436-1-3

doi: 10.32075/17ECSMGE-2019-0852

XVII European Conference
ECSMGE 2019
Reykjavík
on Soil Mechanics
and Geotechnical Engineering

Accounting for nonlinear behavior of ground for the prediction of settlements due to deep excavations

Prise en compte du comportement non linéaire des sols dans l'estimation des tassements des excavations profondes

K. Nejjar[1], R. Witasse[2], D. Dias[3], F. Cuira[1], S. Burlon[1]
[1]*Terrasol, Paris, France*

[2]*Plaxis, Delft, The Netherlands*

[3]*3SR Laboratory Grenoble Alpes University, Grenoble, France*

ABSTRACT: During work progress of a deep excavation, the soil behind the retaining wall undergoes mainly mean effective stress decrease. The volumetric strains generated by sole elastic soil unloading are therefore systematically dilative which induces aberrant ground uplifts. The introduction of plasticity along with a nonlinear elastic domain turns out to be essential for the prediction of ground movements together with realistic wall displacements in the same modeling. A parametric study was carried out using finite element modeling and an advanced soil model called the "Generalized Hardening Soil" which has been recently developed at Plaxis and available as a UDSM (User-Defined Soil Model). It contains the exact same set of features as the well-known "Hardening Soil Small Strain" model but with the advantage of controlling the activation of each mechanism independently. Thus, it makes it possible to identify the mechanisms that affect the most the shape and the amplitude of the ground movements. Numerical results demonstrate that plasticity, being the principal cause for compressive volumetric strains, is not sufficient to compensate the aberrant uplifts due to elasticity. The introduction of strain dependent stiffness is also essential as well as its stress dependency. A back analysis of the extensively documented historical excavation of the Taipei National Enterprise Center validates these findings.

RÉSUMÉ: Lors d'une excavation profonde, le sol derrière l'écran de soutènement subit une diminution de sa contrainte moyenne, les déformations volumiques générées par un sol élastique sont dilatantes induisant ainsi des soulèvements aberrants en surface. L'introduction de la plasticité et la non linéarité du domaine élastique s'avère alors indispensable pour la prédiction de cuvettes de tassements conjointement avec des déformées d'écran réalistes dans une même modélisation. Une étude paramétrique a été réalisée par la méthode des éléments finis grâce à un modèle de sol avancé nommé « Generalized Hardening Soil » récemment développé dans Plaxis est disponible sous la forme d'un USDM (User-Defined Soil Model). Ce modèle reprend toutes les fonctionnalités du modèle « Hardening Soil Small Strain» tout en permettant d'activer ou désactiver indépendamment les différents mécanismes constitutifs du modèle (élastiques et plastiques) impactant l'allure et l'amplitude de la cuvette de tassement.
Les résultats numériques montrent que la plasticité, même si elle est la principale source de déformations volumiques contractantes induisant des tassements, n'est pas suffisante pour compenser les soulèvements aberrants du domaine élastique. L'introduction de la dépendance du module avec la déformation est primordiale en premier lieu suivi de la dépendance du module avec la contrainte moyenne. Une rétro analyse de l'excavation historique du TNEC richement documentée a permis de valider l'ensemble de ces conclusions.

Keywords: Ground settlement; nonlinear soil behavior; deep excavation

1 INTRODUCTION

The expansion of transport network in urban areas, such as the major French project Grand Paris Express, requires an accurate prediction of ground settlements. Tower blocks and high-speed train railways are often close to those deep excavations, hence they are exposed to the induced ground movements. Many empirical methods were developed to estimate the settlement amplitude and profile based on feed-backs from several historical well-documented excavations (Clough et al. 1990, Hsieh et al. 1998, Ou et al. 2011). However, the usefulness of those methods depends on the similitude between features of the current project in terms of soil type and underpinning system and projects that empirical methods used. Thus, numerical modelling becomes essential since it considers all project characteristics and is more qualified to predict relevant results. It provides also a wider choice of soil models that can fit different soil types. Some advanced soil models can be very sophisticated which could discourage engineers since many inputs are required. However, advanced models are necessary to grasp the soil behavior involved in an excavation.

The present paper analyses the "Generalized Hardening soil" recently launched by Plaxis. It contains the exact same set of features as the well-known "Hardening Soil Small Strain" model but with the advantage of controlling the activation of each mechanism independently. Thus, it makes it possible to identify the mechanisms that affect the most the shape and the amplitude of the ground movements. A parametric study is carried out on a theoretical deep excavation and conclusions were used to model the settlement measured for the TNEC excavation.

2 GENERALIZED HARDENING SOIL

During work progress of a deep excavation, the soil behind the retaining wall undergoes mainly mean effective stress decrease. The volumetric strains generated by elastic soil unloading are therefore systematically dilative which induces aberrant ground uplifts. Numerical modeling of such an excavation corresponds to a deactivation of the excavated soil volume which induced immediate elastic uplift. Therefore, an elastic model is clearly not suitable for excavation modelling (Figure 1).

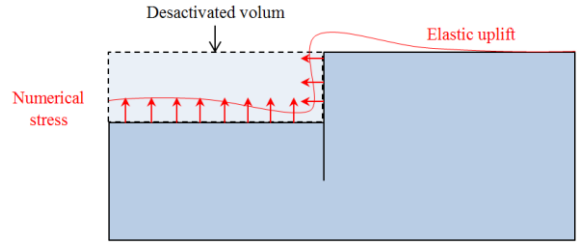

Figure 1: Numerical modelling of an excavation

GHS is an elasto-plastic soil model, with two yield surfaces, cap and shear hardening, a Mohr-Coulomb failure criterion and an elastic domain including strain and stress stiffness dependency (Figure 2). It is a modular model that allows controlling the activation of each mechanism independently.

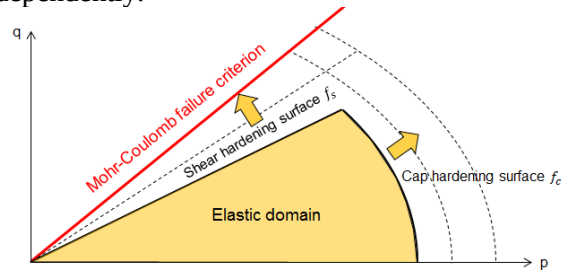

Figure 2: GHS working mechanisms in (p,q) plan

2.1 Elastic domain

2.1.1 Strain stiffness dependency

In the elastic domain, the strain stiffness dependency is provided through the Hardin and Drnevich (1972) sigmoidal model in the form of a shear degradation curve. The latter is presented with the equation 1 where G_0 is the dynamic shear modulus and $\gamma_{0.7}$ is the distorsion reached at 70% of modulus reduction.

$$\frac{G}{G_0} = \frac{1}{1+0.385\frac{\gamma}{\gamma_{0.7}}} \quad (1)$$

The degradation curve has a lower limit modulus G_{ur} (derived from E_{ur} with the Poisson coefficient ν_{ur}, Plaxis Manual).

2.1.2 Stress stiffness dependency

The stress stiffness dependency concerns only the lower limit modulus E_{ur}, the user can choose among 3 formulas:

- Original formula of the classical HS model: it involves shear strength parameter as friction angle φ' and cohesion c', which is incoherent since deformation modulus should be independent of strength.

$$E_{ur} = E_{ur}^{ref}\left(\frac{\sigma_3 + c'.\cot(\varphi')}{\sigma^{ref} + c'.\cot(\varphi')}\right)^{m} \quad (2)$$

- Formula with σ_3 and preconsolidation stress p_c: it excludes shear parameters and introduces the preconsolidation stress p_c in order to avoid the huge decrease of soil stiffness in excavated side that witnesses the greater unloading.

$$E_{ur} = E_{ur}^{ref}\left(\frac{\frac{\sigma_3 + p_c}{2}}{p^{ref}}\right)^{m} \quad (3)$$

- Formula with p' and preconsolidation stress p_c: it replaces σ_3 by p' which is coherent since the modulus is isotropic, it is hence logical to be related to isotropic mean stress p'.

$$E_{ur} = E_{ur}^{ref}\left(\frac{\frac{p' + p_c}{2}}{p^{ref}}\right)^{m} \quad (4)$$

In the precedent formulas, the power m, the reference pressures σ^{ref} and p^{ref} are introduced by the user.

The last formula seems the most appropriate and will be used systematically for the present study.

Moreover, stress-dependent stiffness can be updated at the beginning of each calculation phase only or after each calculation step (or load increment). The latter is more precise since it updates after each stress increment, this option will be retained for the following.

2.2 Plastic domain

GHS allows the user to activate separately shear and cap hardening. The formulation of shear hardening includes a deformation modulus E_{50} which correspond to the secant modulus at 50% of strength in a triaxial compression test. The formulation of cap hardening includes a deformation modulus E_{oed} corresponding to the ratio between vertical compression and settlements in oedometer test. Both modulus can be dependent on the updated stress value such as E_{ur}.

3 PARAMETRIC STUDY ON A THEORETICAL DEEP EXCAVATION

In order to analyze the effect of each mechanism on the ground settlement, many configurations of GHS were explored for a theoretical deep excavation in homogeneous soil. Features of each configuration are presented below. All models have the same Mohr-Coulomb failure criterion.

- MC+SS: elastic perfectly plastic model with strain stiffness dependency
- MC+HS: elasto-plastic model with shear hardening and linear elasticity
- MC+ HS +Cap: elasto-plastic model with shear and cap hardening and linear elasticity
- MC+HS+SS: elasto-plastic model with shear hardening and strain stiffness dependency
- MC+HS+SD: elasto-plastic model with shear hardening and stress stiffness dependency
- MC+HS+SD+SS: elasto-plastic model with shear hardening, strain stiffness dependency and stress stiffness dependency

The geometry of the theoretical excavation is inspired from the real geometry of a new station in the Grand Paris Express transport network under construction (Figure 3).

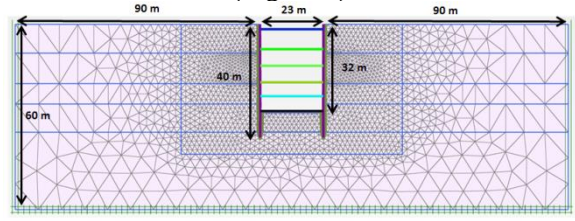

Figure 3: Geometry of the theoretical deep excavation

Table 1 summarizes the standard values of soil parameters used in the present computation.

Table 1: Standard values of soil parameters

E_{50}^{ref}	80 MPa
E_{oed}^{ref}	80 MPa
E_{ur}^{ref}	240 MPa
m	0.3
φ'	30°
c'	0 kPa
G_0	600 MPa
$\gamma_{0.7}$	10^{-4}
ν_{ur}	0.2
K_0	0.5

3.1 Shear hardening effect

In order to obtain meaningful comparison, MC+SS was fitted to MC+HS to give identical stress-strain curve for triaxial compression test using SoilTest simulator in Plaxis. Since the fitting depends on the confining stress, the soil was subdivided to several layers of 3m thickness, and the fitting of each layer was conducted with a constant value of G_0=60.6 MPa and varying $\gamma_{0.7}$. Table 2 summarizes the values retained for each layer for MC+SS.

Table 2: Fitting of MC+SS input parameter $\gamma_{0.7}$ for different subdivided layers

Layer top level	Confining stress	$\gamma_{0.7}$ (10^{-4})
0	30	9.1
3	90	9.1.
6	150	8.5
9	210	7.8
12	270	7.1
15	330	6.5
18	390	5.8
21	450	5.2
24	510	4.5
27	570	3.8
30	630	3.2
33	690	2.5
36	750	1.9
38	810	1.2

Figure 4 presents a comparison between MC+SS and MC+HS for the exacavation problem described in Figure 3. Wall displacements show a perfect fitting between both models, which reflects the quality of the model fitting done before on triaxial compression test. However, large discrepancies are noticed in the ground movements. At 32m depth, MC+HS model presents a coherent settlement whereas MC+SS model shows an aberrant uplift. One can confirm that elastic models produce systematically uplifts and deduce that shear hardening is clearly responsible of the occurrence of settlement.

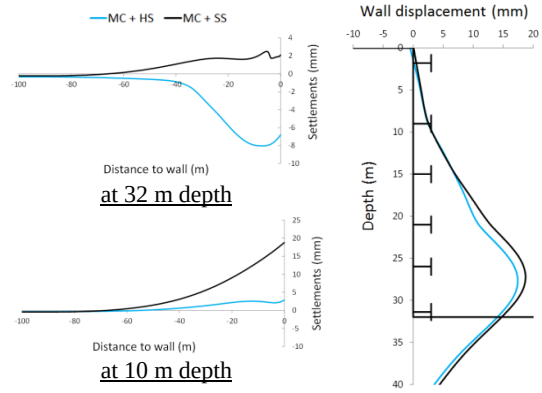

Figure 4: Shear hardening effect on settlement behind wall

Figure 5 and Figure 6 reveals the origin of those differences by showing the compressive and dilative volumetric strains plots. Indeed, MC+HS produces a wider zone (black) of compressive strains whereas MC+SS produces wider dilative zone (white).

However, the performance of the MC+HS configuration is not perfect. Figure 4 shows also the ground movement at 10m depth where both models compute uplift. It means that the produced compressive volumetric plastic strains could not compensate completely for the inevitable elastic dilative volumetric strains. The latter should hence be reduced by considering both

strain and stress stiffness dependency in the elastic domain.

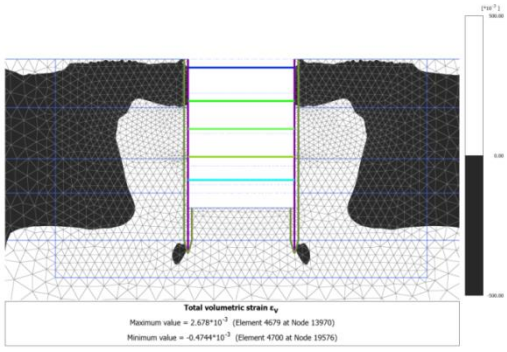

Figure 5: Volumetric deformation for MC+HS model: black zone: compression deformation, white zone: dilative deformation

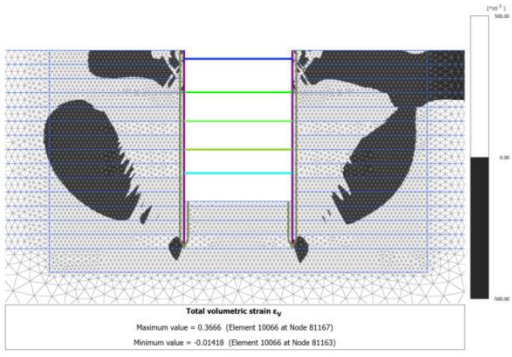

Figure 6: Volumetric deformation for MC+SS model: black zone: compression deformation, white zone: dilative deformation

3.2 Cap hardening effect

Figure 7 shows that the activation of the cap hardening gives the same wall displacements but additional settlements even far from the excavation, which is not relevant. Indeed, the cap hardening takes place when the mean pressure (elastic "trial") exceeds the preconsolidation pressure. In the framework of an excavation problem, the soil behind the wall undergoes mainly a decrease in mean pressure, and consequently the stress paths followed will not hit the cap surface.

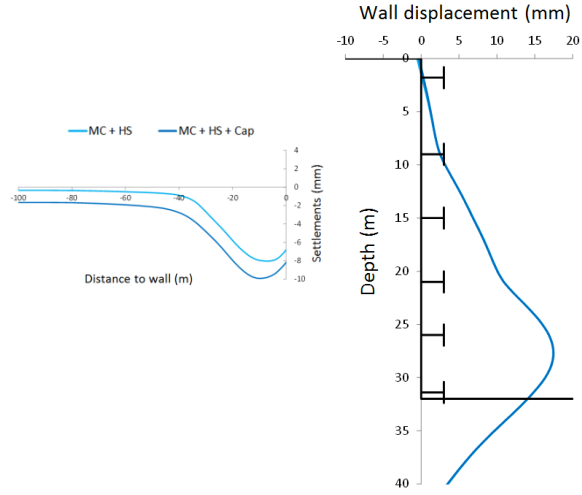

Figure 7: Cap hardening effect on settlement behind wall

Figure 8 shows the locations of cap and shear hardening soil points in both models. The concentration of stress around rigid support by arching effect leads to an increase of the mean pressure which explains the cap hardening points close to wall top. However, the sensitivity of the cap hardening seems high since many cap points are seen far away behind the wall which produces compressive volumetric deformations, hence more settlements.

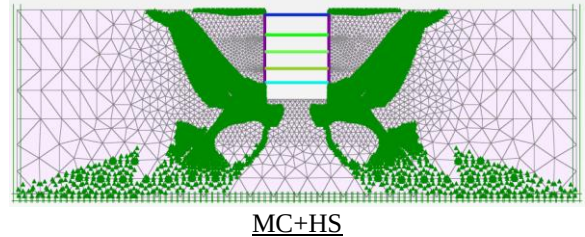

MC+HS

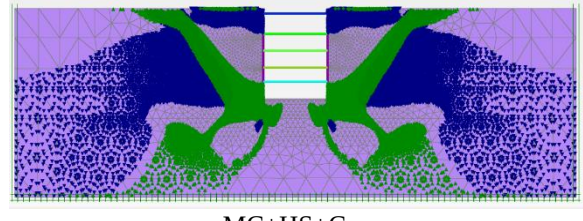

MC+HS+Cap

Figure 8:Cap hardening points (blue) and hardening points (Green) in MC+HS and MC+HS+Cap models

Indeed, cap hardening points are located far from the principal zone of influence. One can conclude that the cap hardening is not useful for excavation case.

3.3 Effect of non-uniform elastic stiffness

Figure 9 presents the results for different GHS configurations at 21 m depth and 32 m depth.

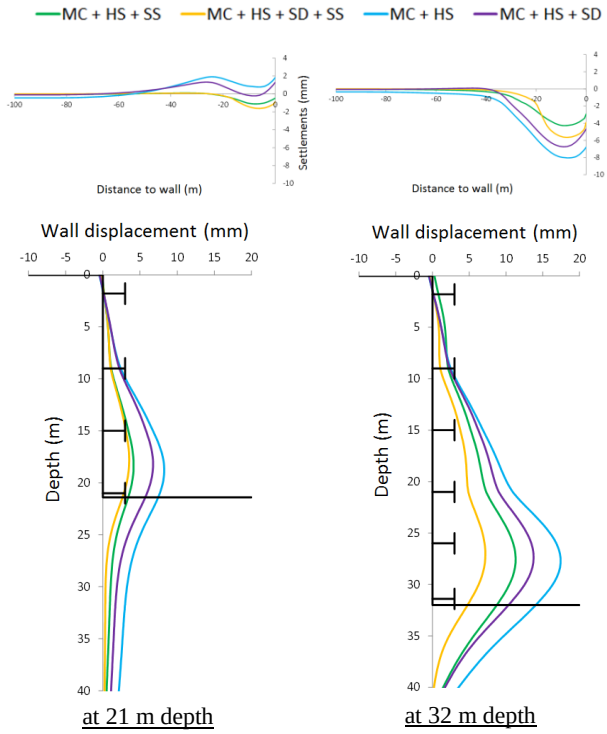

Figure 9: Stress and strain stiffness dependency effect on wall displacements and settlements

At 32m depth, MC+HS model gives the largest settlement and seems satisfactory without any uniform elastic stiffness, however, at 21m depth, the same model shows unrealistic soil uplifts. Actually, the settlements observed at 32m depth are for a very large extend the consequence of the large wall displacement although the model still produces uplift at previous excavation phases.

The comparison between MC+HS, MC+HS+SD, and MC+HS+SS highlights the relevance of stress and strain stiffness dependency. Results obtained at 21m depth shows that the consideration of the strain dependency is essential since the previously observed uplift displacements are eliminated and settlements are obtained instead. The consideration of stress dependency participates in reducing the elastic uplift displacements but seems insufficient for compensating them and producing settlements.

MC+HS+SD+SS presents the combination of those two benefic improvements to the elastic stiffness. At final excavation depth of 32m, MC+HS+SD+SS produces the highest differential displacement (highest slope) which is the most critical aspect for adjacent buildings.

Strain stiffness dependency seems to be the most relevant improvement to be considered. The combination of both strain and stress dependency produces the most plausible settlement shape and the most critical subsidence for nearby infrastructures.

4 APPLICATION TO THE TNEC DEEP EXCAVATION

Taipei National Enterprise Center (TNEC) is a 18-story building with five basement levels. The performance of the 19.7m deep excavation was fully described by Ou et al. (1998) along with soil parameters, detailed construction sequences and instrumentation measurements. Kung et al. (2009) supplemented soil parameters with advanced tests, which allows for a better characterization of their behavior and provide inputs for advanced soil models. Ground movements were measured with regular spacing within a distance of 49m behind the wall, which allows to accurately assess the settlement profile and amplitude.

Stratigraphy is composed of an alternation of thick silty clay layers (CL) and silty sand layers (SM). The substratum is composed of Chingmei Gravel formation. The clay layers have a permeability of 4.10^{-6}cm/s. CL layers are modeled with the undrained A drainage type and

SM layers are modeled as drained materials. The consolidation time is taken from construction sequences as reported by Ou et al. (1998). All soils were modeled with the GHS model except the substratum layer which is modeled as an elastic perfectly plastic soil. Shear parameters are taken from triaxial tests and OCR profile from oedometer tests (Kung et al. 2009). The top 5m of the CL2 layer has been assigned a particular material data set in order to respect the OCR profile. The dynamic shear modulus G_0 is derived from cross hole seismic tests. Its evolution with depth is considered with a fitted power m corresponding to the stress stiffness dependency. The parameter $\gamma_{0.7}$ is derived from advanced triaxial tests with small strain measurements carried out by Kung et al. (2009) on the CL2 layer at different depths. Indeed, the latter measured the ratio between Young modulus at strain level 10^{-4} and 10^{-5} which allows to compute $\gamma_{0.7}$ using Hardin and Drnevich (1972) relationship (equation 1). The computed value was assigned to all layers as a first approach. E_{ur}^{ref} is intentionally taken low in order to let the elastic domain mainly governed by the degradation reduction curve. The moduli E_{50}^{ref} and E_{oed}^{ref} are taken by default equal to half of E_{ur}^{ref}. Table 3 summarizes the soil parameters retained for the different constitutive soil layers.

Table 3: Soil parameters of different layers (Kung et al. 2009)

	φ' (°)	c' (kPa)	OCR	G_0 (MPa)	E_{ur}^{ref} (MPa)	m	$\gamma_{0.7}$
CL1	33	0	4	30	10	0.5	5.0E-5
SM1	31	0	1.85	40	20	0.5	5.0E-5
CL2 Top	30	0	1.43	35	10	1	5.0E-5
CL2	30	0	1.25	35	10	1	5.0E-5
SM2	31	0	1	100	250	0.5	5.0E-5
CL3	32	0	1	100	10	1	5.0E-5
SM3	32	0	1	100	250	0.5	5.0E-5
Gravel	40	40	-	-	200	-	-

Figure 10 shows the geometry and meshing of the Plaxis 2D model.

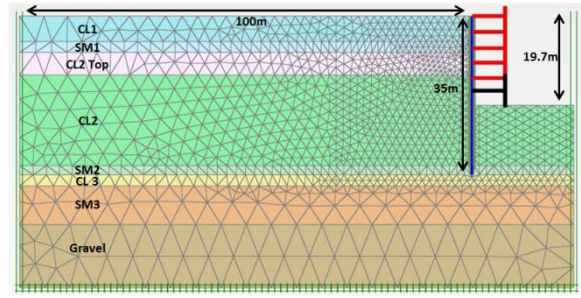

Figure 10: Geometry and meshing of Plaxis 2D model

Figure 11 presents the results obtained with 3 different models (Table 4). The difference between those models concerns only the value of the parameter $\gamma_{0.7}$ since all other parameters come from direct test measurements and CL1 and CL2 layers govern mainly the behavior of the underpinning system.

Table 4: Different values for $\gamma_{0.7}$

$\gamma_{0.7}$	Model 1	Model 2	Model 3
CL 1	5.0 E-5	1.0 E-5	1.0 E-5
CL 2 Top	5.0 E-5	1.0 E-5	1.0 E-5
CL 2	5.0 E-5	1.0 E-5	5.0 E-5

One can see that the variation of $\gamma_{0.7}$ impacts the settlement curve and wall displacements. Model 1 fitted settlements but underestimates wall displacements. Model 2 with reduced $\gamma_{0.7}$ gives greater settlements but better fitted wall displacements. Model 3 reduces only the value of $\gamma_{0.7}$ for shallower layers CL1 and CL2 Top. Settlements and wall displacements seem in better agreement with measurements in that model. Actually having a $\gamma_{0.7}$ increasing with depth is coherent since many experiment approves the same tendency for shear modulus degradation curve for different confining pressure (Seed et al. 1986, Ishibashi et al. 1993). In fact, GHS model could be further improved by adding a stress-dependent $\gamma_{0.7}$. The latter could be beneficial not only to reproduce the increase of $\gamma_{0.7}$ with depth but also its variation with the distance from the wall. Hence the steep slope of measured settlement curve could be properly captured this way. Indeed, soils closer to wall undergo the greater decrease of mean

pressure due to the excavation process. This way a greater decrease of $\gamma_{0.7}$ will lead to lower modulus for the same strain level, which would reproduce even better the narrowness of the settlement trough.

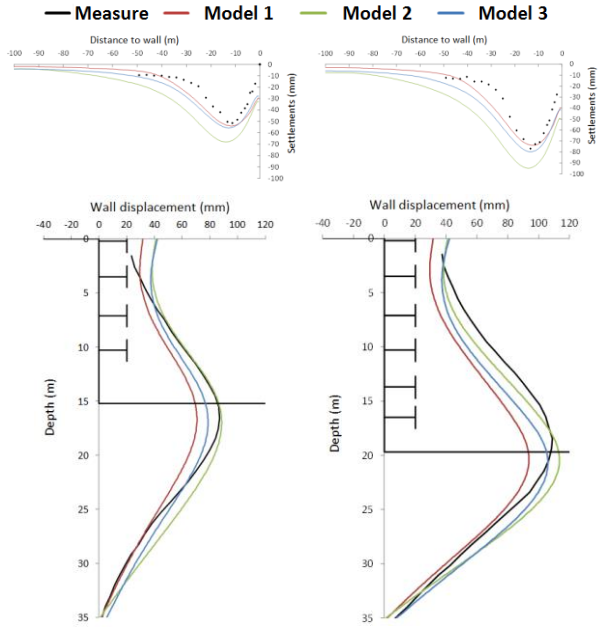

at 15m depth at 19m depth

Figure 11: Comparison between measurements and different models for settlements and wall displacements

5 CONCLUSION

The "Generalized Hardening Soil" is an advanced model that offers a wide choice of model configurations including plastic shear and cap hardening in addition to strain and stress dependent elastic stiffness. The parametric study on a theoretical deep excavation reveals that shear hardening is necessary to produce compressive volumetric strains and hence settlement, however it is not suffisant to compensate the unrealistic linear elastic uplifts. Strain and stiffness dependency contribute to provide more realistic elastic strains. The modelling of TNEC deep excavation approves the consistency of GHS model and highlights the possible improvement of the actual GHS model by adding a dependency between mean pressure and the shape of shear modulus degradation curve through $\gamma_{0.7}$-stress dependency.

6 REFERENCES

Seed H.B., Wong R.T., Idriss I.M., Tokimatsu K. 1986, Moduli and damping factors for dynamic analysis of cohesionnless soils, Journal of Geotechnical Engineering, Vol. 112, N°. 11, pp. 1016-1032

Ishibashi I., Zhang X., 1993, Unified dynamic shear moduli and damping ratios of sand and clay, Japanese Society of Soil Mechanics and Foundation Engineering, Vol. 33, N°. 1, pp. 182-191

Hardin B.O., Drnevich V.P., 1972, Shear modulus and damping in soils: Measurement and parameter effects, Journal of Soil and Mechanics and Foundations Division, Proceedings of the American Society of Civil engineers, 98(SM7), 667-692

Ou C.Y., Liao J.T., Lin H.D., 1998, Performance of diaphragm wall using wall using top-down method, Journal of Geotechnical and Geoenvironmental engineering, pp. 798-808

Kung T.C., Ou C.Y., Juang C.H., 2009, Modelling small-strain behavior of Taipei clays for finite element analysis of braced excavations, Computers and Geotechnics, N°. 36, pp. 304-319

Clough G.W., O'Rourke T.D., 1990, construction induced movements of insitu walls, Design and performance of earth retaining structures Cornell University, ASCE, pp. 439-470

Hsieh P.G., Ou C.Y., 1998, Shape of ground surface settlement profiles caused by excavation, Canadian Geotechnical Journal, N°35, pp. 1004-1017

Ou C.Y., Hsieh P.G., 2011, A simplified method for predicting ground settlement profiles induced by excavation in soft clay, Computers and Geotechnics, N°. 38, pp. 987-997